Revista de Metalurgia
January-March 2023, 59 (1), e234
ISSN-L: 0034-8570
https://doi.org/10.3989/revmetalm.234

Experimental-numerical analysis to determine the efficiency of industrial lubricants in wire drawing process

Thomas Gomes dos Santos[a,*], André Rosiak[a], Diego Rafael Alba[b], Diego Pacheco Wermuth[a], Matheus Henrique Riffel[a], Rafael Pandolfo da Rocha[a], Lirio Schaeffer[a]

[a] Metal Forming Inovation Center CBCM, Federal University of Rio Grande do Sul UFRGS, Porto Alegre, Brasil

[b] Institute for Metal Forming Technology IFU, University of Stuttgart, Stuttgart, Germany

(*Corresponding author: thomas.santos@ufrgs.br)

Submitted: 17 October 2022; Accepted: 6 March 2023; Available On-line: 27 April 2023

ABSTRACT. Drawing is a manufacturing process that consists of indirect deformation by pulling the material through a tool with a conical geometry. The process is usually performed at room temperature (cold forming), so the selection of effective lubricants is critical. If lubrication is inadequate, there is a high risk that both, tool and the manufactured wire, will fail. In this study, annealed AISI 1020 steel rods were drawn and the effectiveness of three different industrial lubricants was tested. During the process, the drawing force values were recorded and used to determine the friction coefficient that developed under each lubrication condition. Numerical simulations were performed to further understand the process. Based on the experimental and numerical results, qualitative and quantitative analysis were performed for each condition. Among the different lubricants used in this study, zinc stearate showed the lowest value for drawing force, 18.8 kN, followed by Lub A and B with values of 20 kN and 20.6 kN, respectively. The numerical models showed excellent approximation to the force values determined in the tests. The values for the coefficient of friction obtained by both the numerical analysis and the empirical model indicate that zinc stearate has the highest lubricating effect among the lubricants focused on this study.

KEYWORDS: Drawing; Efficiency; FEM analysis; Friction; Cold forming

Citation/Citar como: Santos, T.G.; Rosiak, A.; Alba, D.R.; Wermuth, D.P.; Riffel, M.H.; Rocha, R. P.; Schaeffer, L. (2023). "Experimental-numerical analysis to determine the efficiency of industrial lubricants in wire drawing process". *Rev. Metal.* 59(1): e234. https://doi.org/10.3989/revmetalm.234

RESUMEN: *Análisis numérico-experimental para determinar la eficiencia de lubricantes industriales en el proceso de estirado.* El estirado es un proceso de fabricación que consiste en la deformación indirecta tirando del material a través de una herramienta de geometría cónica. El proceso generalmente se lleva a cabo a temperatura ambiente (formado en frío), por lo que la selección de lubricantes efectivos es fundamental. Si la lubricación es inadecuada, existe un alto riesgo de que tanto la herramienta como el alambre fabricado fallen. En este estudio, se estiraron varillas de acero AISI 1020 recocidas y se probó la efectividad de tres lubricantes industriales diferentes. Durante el proceso, los valores de la fuerza de tracción se registraron y utilizaron para determinar el coeficiente de rozamiento desarrollado bajo cada condición de lubricación. Se realizaron simulaciones numéricas

para comprender mejor el proceso. Con base en los resultados experimentales y numéricos, se realizaron análisis cualitativos y cuantitativos para cada condición. Entre los diferentes lubricantes utilizados en este estudio, el estearato de zinc presentó el menor valor de fuerza de tracción, 18,8 kN, seguido de Lub A y B con valores de 20 kN y 20,6 kN, respectivamente. Los modelos numéricos mostraron una excelente aproximación a los valores de fuerza determinados en las pruebas. Los valores del coeficiente de rozamiento obtenidos tanto por análisis numérico como por el modelo empírico indican que el estearato de zinc tiene el mayor efecto lubricante entre los lubricantes objeto de este estudio.

PALABRAS CLAVE: Análisis MEF; Estirado; Eficiencia; Formado en frío; Rozamiento

ORCID ID: Thomas Gomes dos Santos (https://orcid.org/0000-0002-6570-4872); André Rosiak (https://orcid.org/0000-0002-7162-5169); Diego Rafael Alba (https://orcid.org/0000-0001-8321-5872); Diego Pacheco Wermuth (https://orcid.org/0000-0003-0557-2385); Matheus Henrique Riffel (https://orcid.org/0009-0009-4639-0431); Rafael Pandolfo da Rocha (https://orcid.org/0009-0004-7835-5159); Lirio Schaeffer (https://orcid.org/0000-0002-3427-2405)

1. INTRODUCTION

Drawing is a forming technique aimed to reduce the cross-section and thus increasing the material in the longitudinal direction. The technique consists in drawing the raw material at the exit of a die, which determines the geometry of the final product (Schaeffer, 2004). Generally, the drawing process is carried out cold, although a significant temperature rise in the material is observed due to the work of deformation (Dieter, 1981)

Knowledge of the geometric parameters shown in Fig. 1a is essential for performing the procedure. During drawing, stresses in the longitudinal (σz), radial (σr), and tangential (σt) directions act on the formed rod. These stresses are shown schematically in a simplified form in Figure 1b.

Many process variables affect the quality of the manufactured wires. Various researchers have studied the effects of variables such as the reduction ratio (r), the half-angle of the mould (α), and the friction coefficient (μ) (Dixit and Dixit, 1995). De Castro *et al.* (1996) analyzed the effects of the half-angle of the dies on the mechanical properties of annealed copper bars. Norasethasopon and Yoshida (2006) studied the effects of non-metallic inclusions and stress states generated during drawing of threaded copper wires. Vega *et al.* (2009) measured temperature and drawing force by changing the drawing speed and simultaneously measuring the drawing force behind the die with a wire roll gauge.

The friction coefficient presents between the working material and the surface of the tool has a direct influence on the final result of the product (Santos *et al.*, 2022). For this reason, the choice of a suitable lubricant is of great importance. Insufficient lubrication negatively affects the surface quality of the drawn bar, increases the required effort and accelerates the wear mechanisms in the die (Bresciani *et al.*, 1986)

Residual stresses in the drawn products have a significant influence as they affect the occurrence and development of surface cracks in the wire (Överstam, 2006; Ajiboye *et al.*, 2010). Studies show that the temperature and the drawing force depend on the interfacial conditions.

Quantifying the friction generated in the process by defining the coefficient of friction allows qualitative analysis of different lubricants and optimization of the process (Wistreich, 1955; Moon and Kim, 2012).

Several authors have already used inverse finite element analysis to determine the coefficient of friction that arises during the mechanical forming processes (Platov *et al.*, 2017). In this approach, the forming force is first recorded experimentally. Then, the forming force is calculated by several numerical models of the process in which all boundary conditions are kept constant except for the friction coefficient. This parameter is varied in each model within the range predicted for the process under study. The forming force obtained in each model is compared

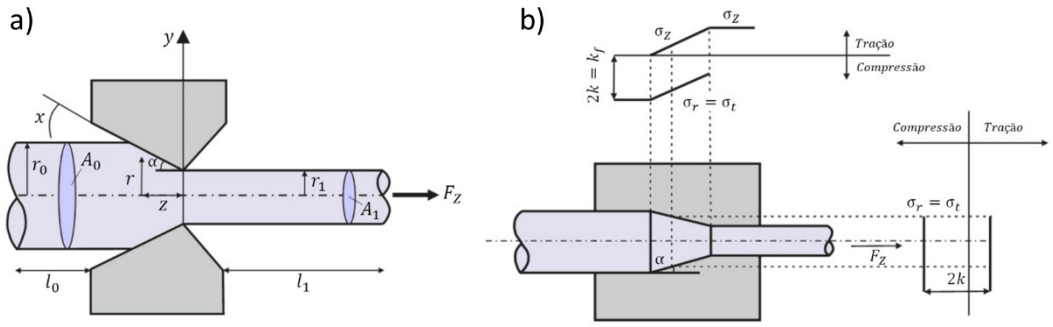

Figure 1. a) Geometric parameters in drawing, b) Simplification of tensions in drawing, Schaeffer (2004).

with the experimental result. The convergence between numerical and experimental data gives the coefficient of friction of the physical process. In this study, a methodology is proposed to quantify the performance of different lubricants in the drawing process. In parallel with the experimental procedure, inverse finite element analyzes were performed to determine the friction coefficients for each physical experiment. Empirical models were used in the physical experiments to determine the coefficient of friction, i.e., the model proposed by Siebel. The friction coefficient values were used to evaluate the ability of each lubricant to mitigate friction in the drawing process.

2. MATERIALS AND METHODS

2.1. **Material**

In the experimental procedure, specimens were drawn from the annealed AISI 1020 carbon steel. The chemical analysis of the material obtained by optical spark emission spectrometry is shown in Table 1. The composition is within the nominal range reported in the literature (ASM Handbook, 2004).

In the annealing treatment, the material was heated in a resistance furnace at 850 °C for 1 hour for complete temperature homogenization and then slowly cooled in the furnace. The final microstructure, after annealing, is shown in Fig. 2 and consists of a large proportion of ferrite with dispersed pearlite grains, which is a typical microstructure of low carbon steels.

To evaluate the microstructure obtained, metallographic specimens were prepared according to standard procedures (ASM Handbook, 2004) and etched by immersion in a 5% Nital solution for 10 seconds. The mechanical behavior of the annealed material was studied by tensile tests according to the procedure standardized in ASTM E8 (2013), Appendix A.

Table 1. Result of chemical analysis of AISI 1020 steel (% mass)

C	Mn	P	S	Si	Cr	B	Ti	Al
0.23	1.24	0.02	0.002	0.21	0.19	0.0039	0.046	0.037

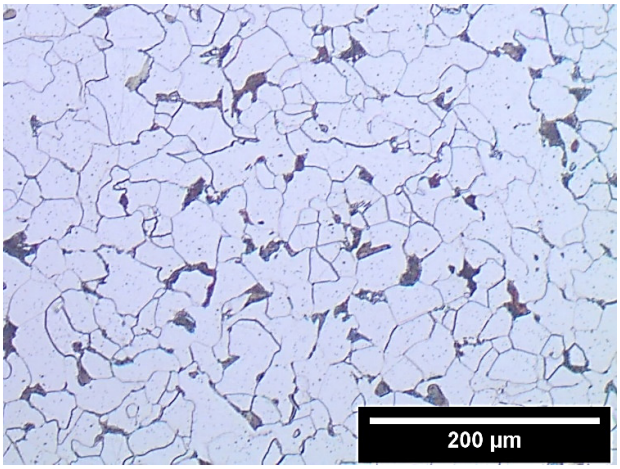

Figure 2. Microstructure of AISI 1020 steel after annealing.

2.2. Drawing Test

Figure 3 shows the dimensions of the die and the specimens used for the drawing tests. The end sections of the specimens were sharpened to facilitate fixation and to limit the length of the area to be drawn to 100 mm.

Drawing tests were carried out on a universal testing machine EMIC DL6000, with a load capacity of 600 kN. The process speed was set at 60 mm·min^{-1}. During the tests, displacement and force measurements were recorded. Figure 4 presents the scheme used to carry out the drawing experiments.

To perform the experiments, the test specimens (Fig. 3b) were wrapped in lubricant (Table 2) to cover the entire area to be drawn. The three lubricants listed in Table 2 were used for the experiments.

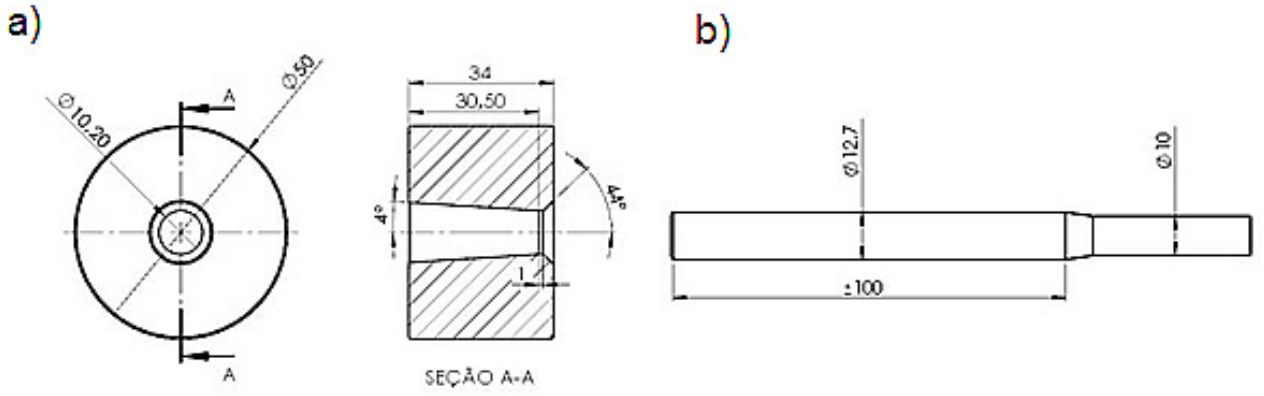

Figure 3. Dimensions of (a) die and (b) specimens.

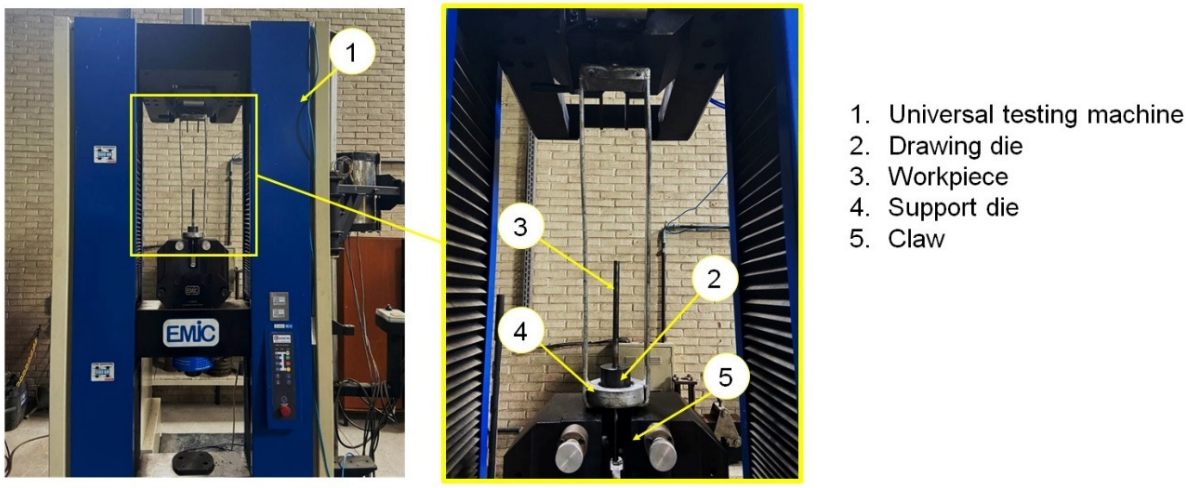

Figure 4. Schematic view of the drawing experiments.

Table 2. Lubricants used in experiments

Lubricant	Characteristic	Application status
Zinc Stearate	Soap	Power
Lub. A	Polyglycol - Synthetic lubricant	Oil
Lub. B	Paraffinic - Mineral lubricant	Oil

2.3. Determination of the Friction Coefficient

Siebel (1947) proposed an analytical model for estimating the forming force (F) in drawing operations. The model relates the average yield stress (k_{fm}), the tool angle (α), the friction coefficient (μ), and the initial (A_0) and final (A_1) surfaces of the wire rod. The drawing force is mathematically expressed by Eq. (1):

$$F = A_1 \cdot k_{fm}\left[ln\left(\frac{A_0}{A1}\right) + \left(\frac{2\alpha}{3}\right) + \left(\frac{\mu}{\alpha} ln\left(\frac{A_0}{A_1}\right)\right)\right] \quad (1)$$

Equation (1) is used to determine the friction coefficient for each condition studied. With the experimental data, all variables of the equation are defined and the value of μ can be isolated and calculated.

Inverse Finite Element Analysis

As it is presented in Fig. 5, for the inverse analyzes, numerical models using the finite element method (FEM) were created in the Forge NxT 3.2 software, Fig. 6. The models consisted of using the experimentally determined values of the drawing force (F_{exp}) and its definition as a target to be achieved in the models, in the following objective function to be minimized (Alba *et al.*, 2018).

$$T_{obj} = \sum_{i=1}\left(F_{exp(i)} - F_{sim(i)}\right)^2 \quad (2)$$

Here, F_{sim} is the value obtained from the drag force via the FEM model. Thus, the objective function in this study is defined as the sum of the squares of the errors between the experimental drag force and the via FEM, where the objective is to obtain the lowest values of the T_{obj} function.

For this, the values for the friction coefficients were determined to satisfy the condition for the difference between the values of the experimental and numerical force, equation two.

To reduce the computational effort, only the behavior of the specimens was classified as viscoplastic and the tools were kept as rigid. The yield curve determined experimentally in the tensile test was introduced into the software to characterize the mechanical behavior of the material. Table 3 lists the boundary conditions used in the numerical models.

The average value of the drawing force monitored in the experiments is used for the inverse analysis strategy. The friction coefficient for each test is determined by this value.

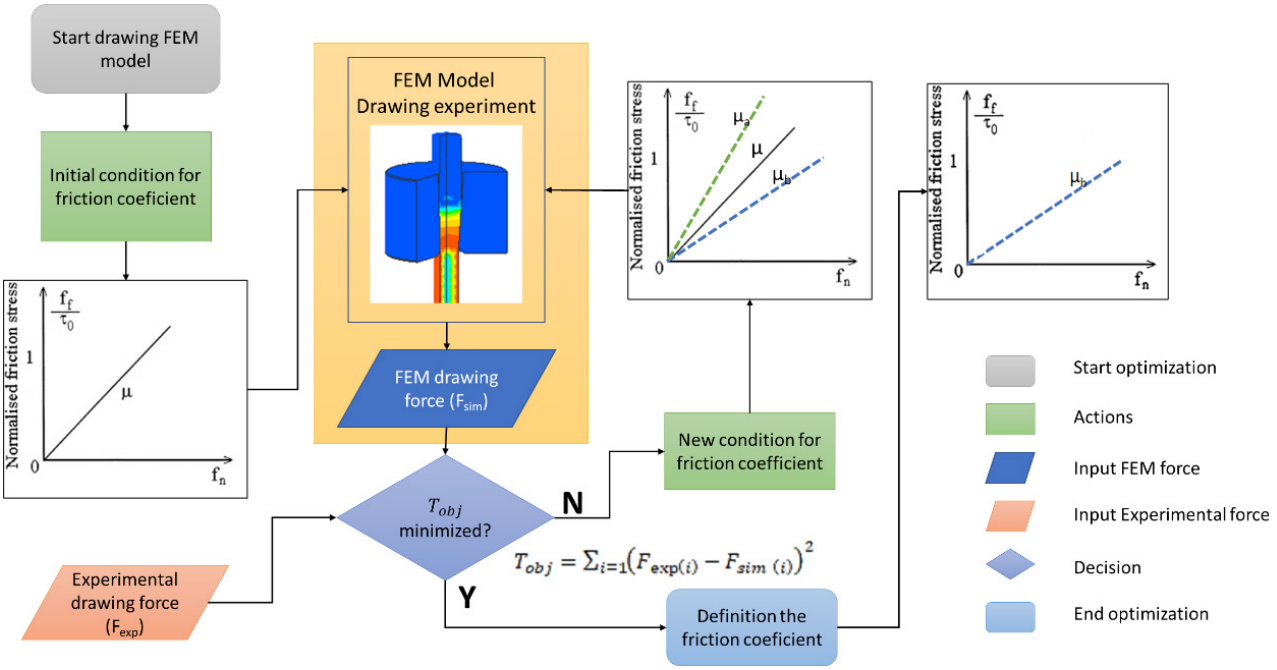

Figure 5. Defined optimization strategy for the numerical models.

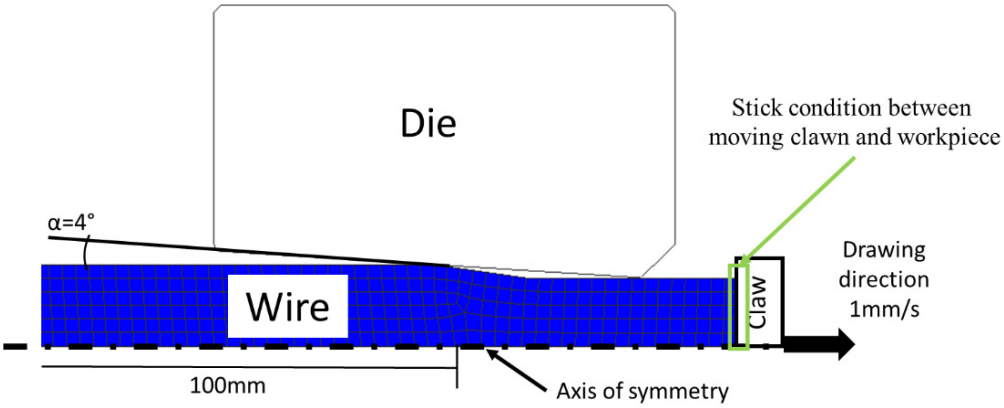

Figure 6. Numerical model of the drawing process.

Table 3. Input data used in numerical models

Type analysis	2D viscoplastic
Number of elements	852
Node number	3408
Element size	0-9837 mm
Element type	Quadrilateral
Tool temperature	20 °C
Initial temperature of specimen	20 °C
Drawing speed	60 mm·min^{-1}
Heat transfer coefficient	10000 W·m^{2}K^{-1}

3. RESULTS

3.1. Initial Characterization

The flow curve of the annealed steel AISI 1020 determined in the uniaxial tensile test is presented in Fig. 7.

In addition, Fig. 7 shows the flow curve based on the Hollomon formulation, which describes the mechanical behavior of the material during cold plastic deformation (Hollomon, 1945). It can be observed that the curve arising from the equation correlates with good agreement to the experimental results. Furthermore, through the tensile test performed, it

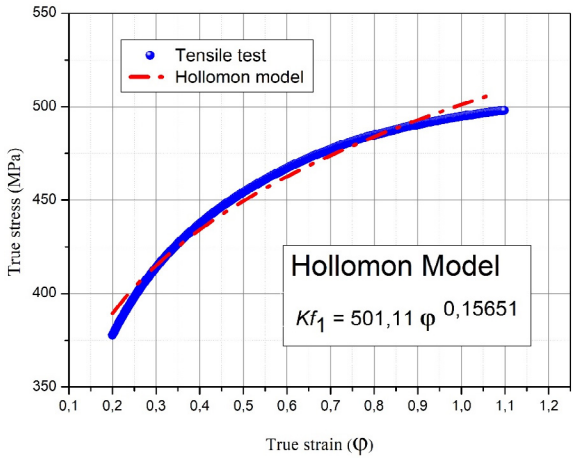

Figure 7. Flow curve obtained by the Tensile Test governed by NBR6152.

Table 4. Mechanical properties of annealed AISI 1020 steel

Yield stress (MPa)	Ultimate Tensile stress (MPa)	Elongation A (%)	Reduction in area Z (%)
218.6	341.0	37.0	21.8

is possible to obtain relevant information about the material. Table 4 shows other properties evaluated from the test.

3.2. Drawing Tests

Figure 8 shows the development of the drawing force as a function of time, which was determined experimentally for each investigated condition.

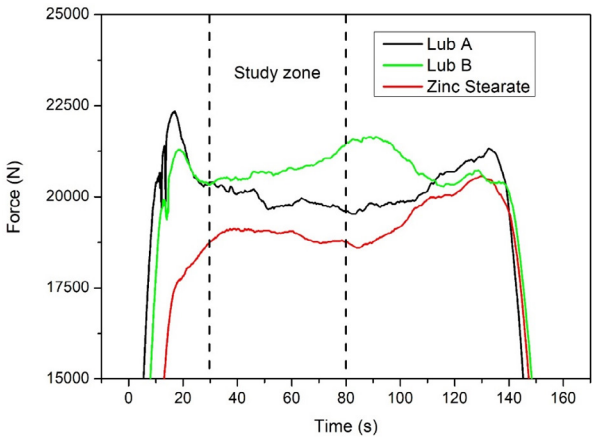

Figure 8. Drawing force values obtained in the experiments, and defined study region.

The drawing force values were subject to fluctuations caused by the surface condition of the specimens. This behavior is due to the change in the lubrication regime, which initially migrates from static friction to sliding friction. In the experiments where stearate was used as a lubricant, it was found that the drawing force values were lower than those obtained with lubricants A and B. Regarding the curve of force versus time, it was noted that the drawing force remained constant until approximately 80 seconds of drawing, after which, there was a gradual increase until reaching the maximum value at the end of the drawn bar. In the tests carried out with lubricants A and B, it was observed that the drawing force presented significant oscillations, with an initial peak in both cases, due to the beginning of the process in which the fluid does not completely cover the work surface, resulting in a dry lubrication regime, affecting the state of application of lubricants. After the initial peak of force, the lubrication regime changed from static to mixed, leading to a reduction in force value. With regard to lubricant A, the force value remained reduced after the start until about 80 seconds, from which the drawing force increased until the end of the process. In the case of lubricant B, a more pronounced increase in the force was observed up to about 90 seconds, after which the force value dropped again. Such oscillations and changes in the lubrication regime can be explained by the variation in the contact pressure, which is a highly sensitive factor in liquid lubricants, causing a change in the thickness of the lubricating film at high contact pressures, something frequent in cold drawing processes.

The region of the curves where the oscillations were smaller was selected as the analysis area for the determination of the coefficients of friction.

3.3. Determination of the Coefficient of Friction

Analytical Approach

Table 5 lists the process variables that were experimentally defined for each studied condition.

Using the data in Table 5, the drawing force for each condition studied was calculated using Eq. (1). Figure 9 compares the experimental force results with the Siebel model results.

Table 5. Process variables defined experimentally for each condition analyzed

Condition	Force, F [N]	Average Yield Stress, k_{fm} [MPa]	Tool Angle, α [Rad]	Initial area, A_0 [mm²]	Final area, A_1 [mm²]
Zinc Stearate	18899.2	218.6	0.0698	126.7	81.7
Lub A	20035.4				
Lub B	20662.7				

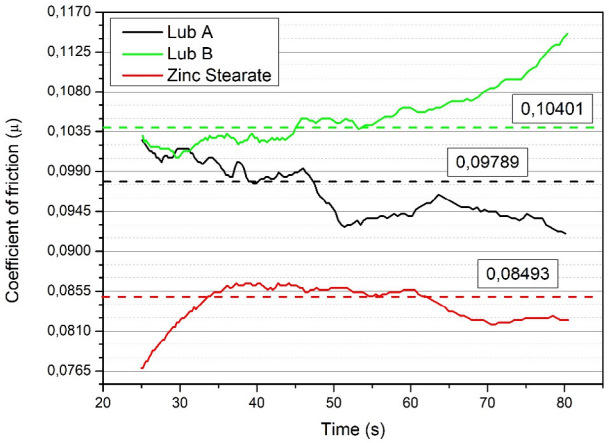

Figure 9. Values of the coefficient of friction obtained from the Siebel Model.

Inverse Finite Element Analysis

Figure 10 shows the development of the drawing force as a function of time, which was determined numerically and experimentally.

The value of the actual stress for each case can be seen in Fig. 11, where it can be observed that in all cases there are stresses of not less than 295 MPa at the beginning of the drawing process. It can also be observed that after the bar is drawn, the stresses near the core are of the order of 130 MPa, being higher when Lub B is used and lower when Stearate is used. Figure 12 shows this effect in detail for each lubricant tested.

The maximum stress and strain values were observed on the drawn surface. The maximum true strain observed in the three conditions is equal and

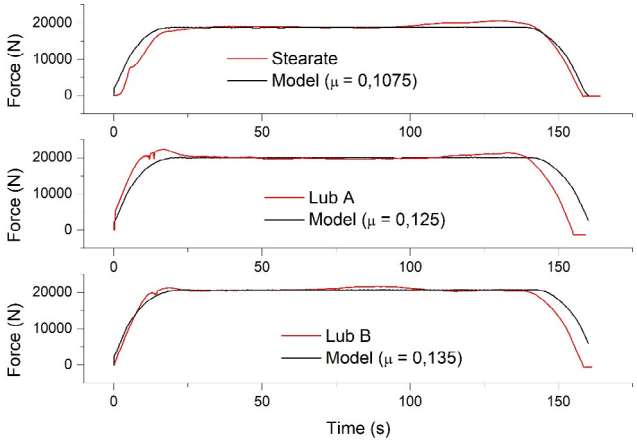

Figure 10. Drawing force values obtained by the simulation models.

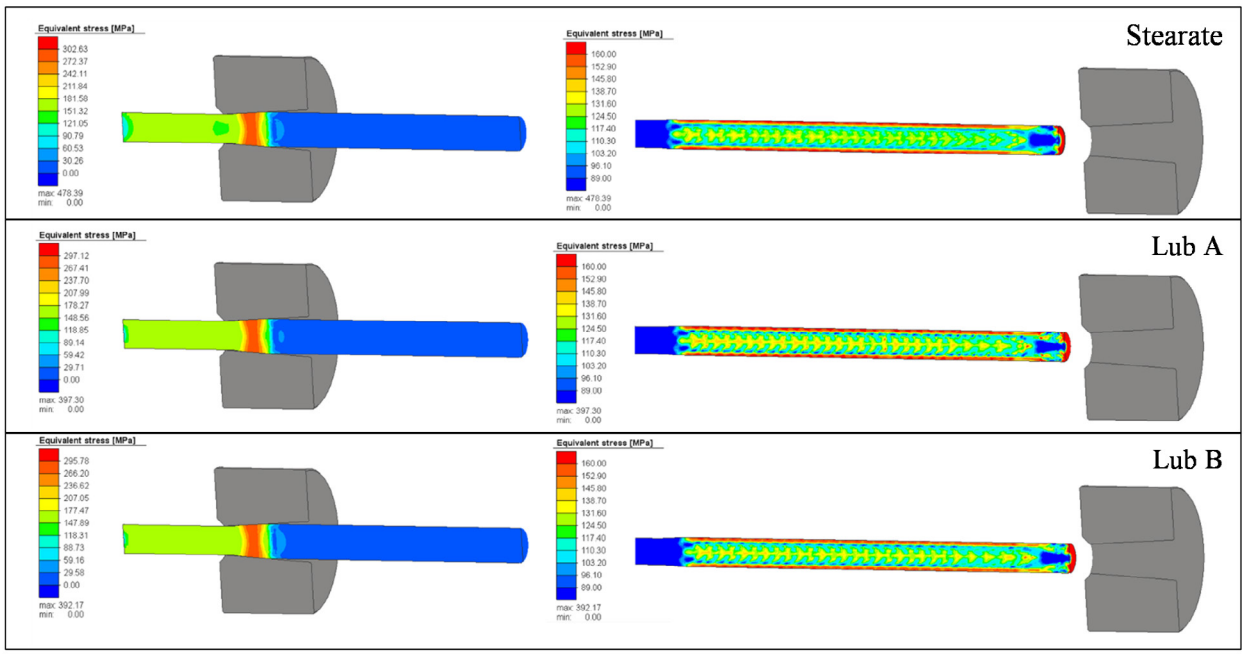

Figure 11. True stress values at the beginning and after each wire drawing experiment.

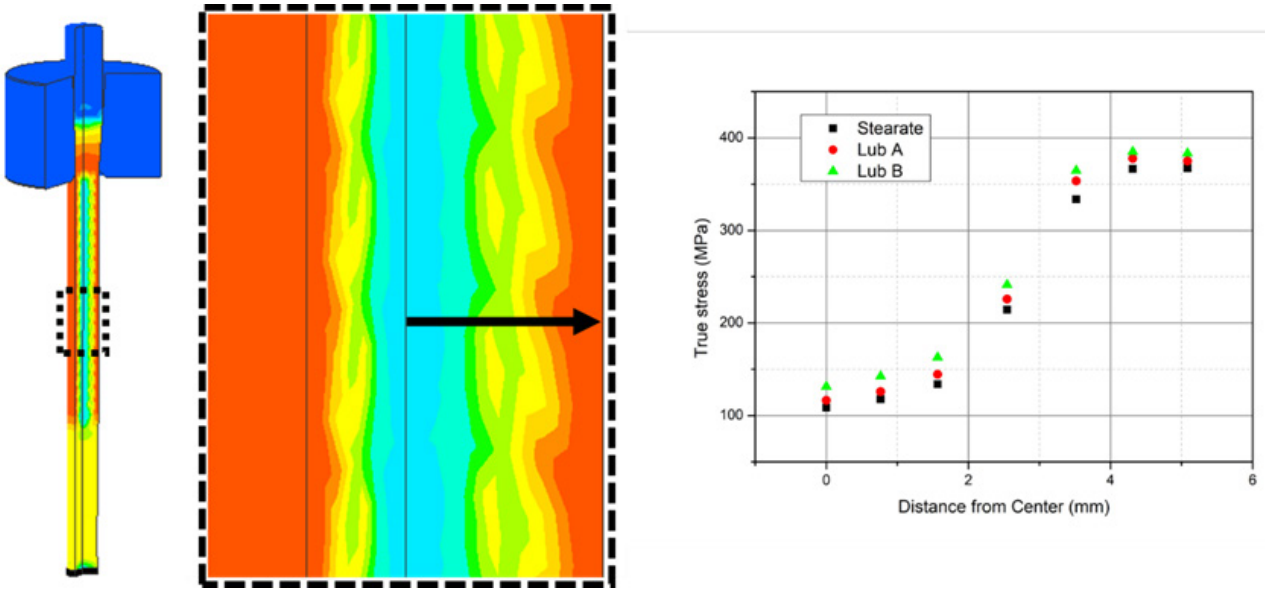

Figure 12. True stress distribution from the center of the drawn bar.

corresponds to 0.36. The magnitude of the maximum equivalent voltage is different under each condition. This demonstrates that the lubrication has an effect on the stresses developed in the process. In condition 1 (stearate) a maximum stress value of 478.4 MPa was observed. In condition 2 (Lub A), 397.3 MPa and in condition 3 (Lub B) 392.2 MPa. The average value of the 3 conditions is 422.6 MPa. The stress-strain relationship verified in the simulations coincides with the stress-strain curve shown in Fig. 7, showing a difference of 1% between the values.

In Fig. 13, the true strain data can be observed evidencing the strain distribution in the drawn region, being smaller near the core and larger on the surface.

An analysis of the maximum temperature during drawing can be seen in Fig. 14. The maximum tem-

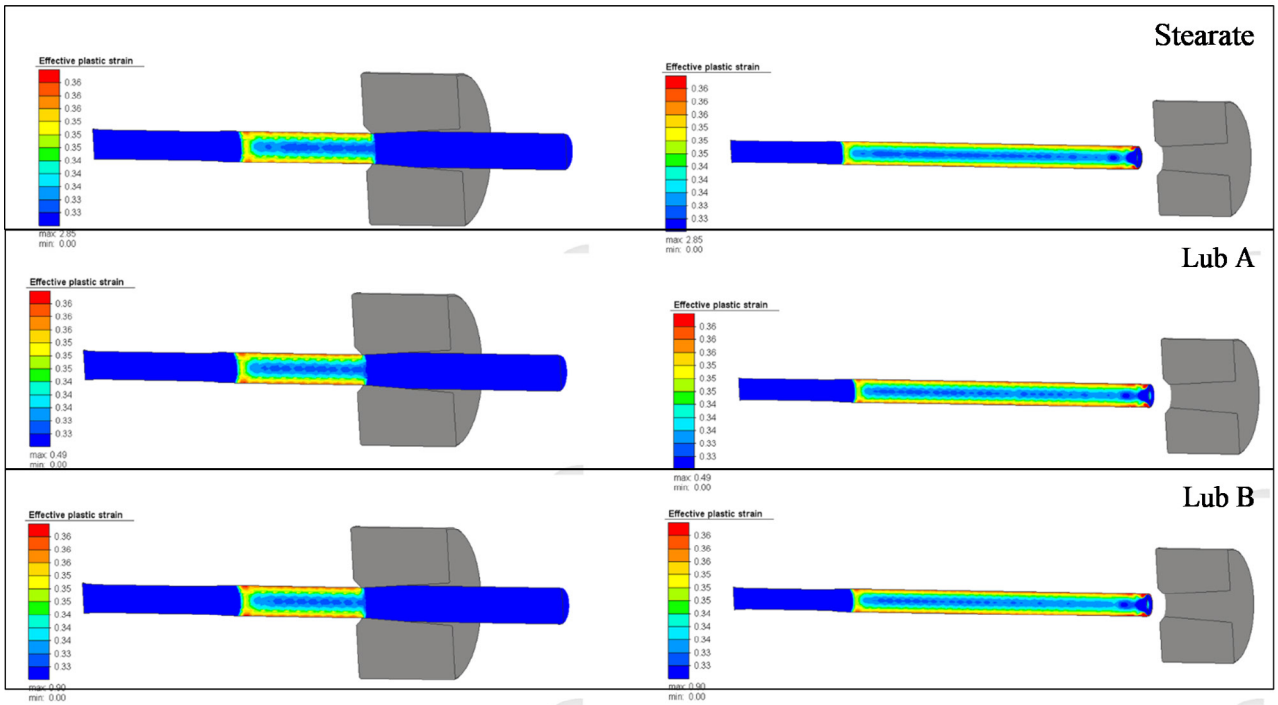

Figure 13. True strain values, during and after each wire drawing experiment performed.

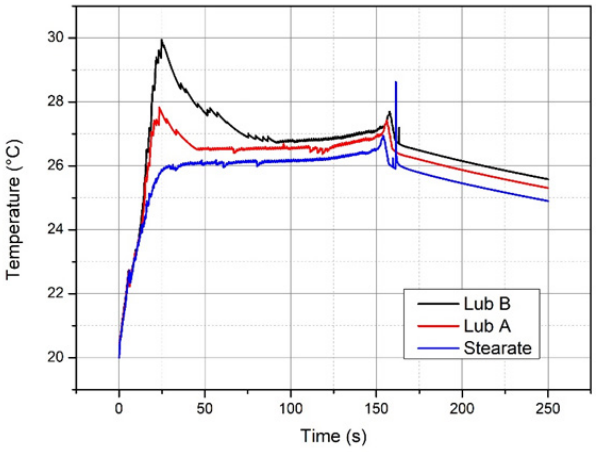

Figure 14. Maximum temperature values obtained in the FEM models.

perature was located on the drawing surface near the exit of the die. It shows a correlation with the values of the coefficient of friction, since higher temperatures were found in conditions with greater friction, as noted by Vega *et al.* (2009). When Stearate was used, the temperature values were the lowest compared to the two cases with Lub A and B, which proves the influence on this property as well as on the drawing force values.

4. DISCUSSION

The coefficients of friction obtained by the analytical and numerical approach are shown in Table 6. The experimentally determined force data (Fig. 8) show that there were variations in the force values for all the drawing procedures analyzed. It is believed that the change in lubrication regime and the presence of surface defects in the specimens from the annealing process contribute to this behavior.

Table 6. Friction coefficient values obtained analytically and through inverse analysis

Lubricant	Coefficient of friction [μ]		Relative error [%]
	Siebel	Numerical Model	
Zinc Stearate	0.08493	0.1075	26.57
Lub A	0.09789	0.125	27.69
Lub B	0.10401	0.135	26.44

5. CONCLUSIONS

– Zinc stearate was the lubricating method that gave the lowest drawing force in the experiments and had a maximum force value of 18,899 kN. Forming with lubricants A and B resulted in maximum forces of 20,035 and 20,662 kN, respectively. Force is a process-dependent variable, and the maximum value obtained during forming depends on independent variables such as friction. The lower force required for forming with zinc stearate indicates that this lubricant presents a higher effectiveness in reducing friction between contact surfaces.
– The Siebel Model was able to reproduce the variations in the values of the drawing force, and among the lubricants, zinc stearate was the one that had the lowest average value of the coefficient of friction of 0.08493.
– The numerically determined tensile force values showed excellent correlation with the experimental values with maximum deviations of 0.5%.
– Among the analytical and numerical methods, the numerical method presents a conservative behaviour, defining higher values for the friction coefficients when compared to those determined by the numerical model.
– The results calculated with the finite element method and the Siebel model show a maximum relative error of 27.69%. However, from a qualitative point of view, both approaches show convergences that define zinc stearate as the most suitable lubrication method, followed by lubricant A and B, respectively.
– The insufficient performance shown by lubricants A and B may be related to their formulation, composition and their physical and chemical characteristics, which may not be consistent with the drawing process in question. In addition, there is the possibility of compatibility problems between the lubricant and the material to be drawn, culminating in unsatisfactory performance of the lubricant. In this sense, it is imperative to continue the research and development of new lubricants, with a view to finding alternatives that are more compatible with the drawing process.

ACKNOWLEDGMENTS

This study was financed in part by the Conselho Nacional de Desenvolvimento Científico e Tecnológico – Brasil (CNPq) – Finance Code CNPq/MCTI/FNDCT nº 18/2021 (Process: 404196/2021-7). The authors are recipients of fellowships from the CNPq (research productivity – PQ1-4/2021; PDJ – 25/2021; GD – 2019) and CAPES (PROEX-IES-2020).

REFERENCES

Ajiboye, J.S., Jung, K.H., Im, Y.T. (2010). Sensitivity study of frictional behavior by dimensional analysis in cold forging.

J. Mech. Sci. Technol. 24, 115-118. https://doi.org/10.1007/s12206-009-1202-x.

Alba, D.R., Santos, T.G., Schaeffer, L. (2018). Otimização em elementos finitos para definição do fator de atrito através de ensaios de compressão de anéis. 22nd International Forging Conference, 38 SENAFOR, Brazil.

ASM Handbook (2004). *Metallography and Microstructure*. Volume 9, ASM International, Materials Park, George F. Vander Voort (Editor), OH, USA.

ASTM E8 (2013). Tensile Testing of Metals. ASTM International, West Conshohocken, PA, USA.

Bresciani, F.E., Zavaglia, C.A.C., Nery, F.A.C., Button, S.T. (1986). *Conformação Plástica dos Metais*. V.2, Editora Unicamp.

De Castro, A.L.R., Campos, H.B., Cetlin, P.R. (1996). Influence of die semi-angle on mechanical properties of single and multiple pass drawn copper. *J. Mater. Process. Technol.* 60 (1-4), 179-182. https://doi.org/10.1016/0924-0136(96)02325-4.

Dieter, G.E. (1981). *Metalurgia Mecânica*. 2ª Edição, Editora Guanabara.

Dixit, U.S., Dixit, P.M. (1995). An analysis of the steady-state wire drawing of strain-hardening materials. *J. Mater. Process. Technol.* 47 (3-4), 201-229. https://doi.org/10.1016/0924-0136(95)85000-7.

Hollomon, J.H. (1945). Tensile deformation. *Trans. Metall. Soc.* AIME, 162, 268–290.

Moon, C., Kim, N. (2012). Analysis of wire-drawing process with friction and thermal conditions obtained by inverse engineering. *J. Mech. Sci. Technol.* 26 (9), 2903-2911. https://doi.org/10.1007/s12206-012-0711-1.

Norasethasopon, S., Yoshida, K. (2006). Influences of inclusion shape and size in drawing of copper shaped-wire. *J. Mater. Process. Technol.* 172 (3), 400-406. https://doi.org/10.1016/j.jmatprotec.2005.09.020.

Överstam, H. (2006). The influence of bearing geometry on the residual stress state in cold drawn wire, analyzed by the FEM. *J. Mater. Process. Technol.* 171 (3), 446-450. https://doi.org/10.1016/j.jmatprotec.2005.08.012.

Platov, S.I., Nekit, V.A., Ogarkov, N.N. (2017). Determination of Frictional Forces during Wire Rod Drawing Process by Reverse Method. *Solid State Phenom.* 265, 1152–1156. https://doi.org/10.4028/www.scientific.net/SSP.265.1152.

Santos, T.G., Alba, D.R., Schaeffer, L. (2019). Análise do desempenho de diferentes modelos de atrito na simulação numérica do processo de forjamento isotérmico. 23nd International Forging Conference, 39 SENAFOR, Brazil.

Schaeffer, L. (2004). *Conformação Mecânica*. 2ª edição, Imprensa Livre Editora, Porto Alegre.

Siebel, E. (1947). Der decretage Stand der Erkenntnisse über Die Mechanischen beim Drahtziehen. *Stahl und Eisen* 11–12, 171-204. https://delibra.bg.polsl.pl/Content/48253/BCPS_52703_1947_Stahl-und-Eisen--Jg-.pdf

Vega, G., Haddi, A., Imad, A. (2009). Temperature effects on wire drawing process: experimental investigation. *Int. J. Mater. Form.* 2 (Suppl. 1), 229-232. https://doi.org/10.1007/s12289-009-0468-y.

Wistreich, J.G. (1955). Investigation of the Mechanics of Wire Drawing. *Proc. Inst. Mech. Eng.* 169 (1), 654–678. https://doi.org/10.1243/PIME_PROC_1955_169_070_02.